

Deep Gated Recurrent and Convolutional Network Hybrid Model for Univariate Time Series Classification

Nelly Elsayed, *Student Member, IEEE*, Anthony S. Maida and Magdy Bayoumi, *Life Fellow, IEEE*

Abstract—Hybrid LSTM-fully convolutional networks (LSTM-FCN) for time series classification have produced state-of-the-art classification results on univariate time series. We show that replacing the LSTM with a gated recurrent unit (GRU) to create a GRU-fully convolutional network hybrid model (GRU-FCN) can offer even better performance on many time series datasets. The proposed GRU-FCN model outperforms state-of-the-art classification performance in many univariate and multivariate time series datasets. In addition, since the GRU uses a simpler architecture than the LSTM, it has fewer training parameters, less training time, and a simpler hardware implementation, compared to the LSTM-based models.

Index Terms—GRU-FCN, LSTM, fully convolutional neural network, time series, classification

I. INTRODUCTION

A time series (TS) is a sequence of data points obtained at successive equally-spaced time points, ordinarily in a uniform interval time domain [1]. TSs are used in several research and industrial fields where temporal analysis measurements are involved such as in signal processing [2], pattern recognition [3], mathematics [1], psychological and physiological signals analysis [4], [5], earthquake prediction [6], weather readings [7], and statistics [1]. There are two types of time series: univariate and multivariate. The multivariate time series is more intricate and complex than the univariate time series because it has multiple varying variable dependencies over a period of time but the univariate has only one varying variable over time [1]. In this paper, we study the univariate time series classification.

There have been several approaches to time series classification. The distance-based classifier based on the k-nearest neighbor (KNN) algorithm is considered a baseline technique for time series classification. Mostly, distance-based classifier uses Euclidean or Dynamic Time Wrapping (DTW) as a distance measure [8]. Feature-based time series classifiers are also widely used such as the bag-of-SFA-symbols (BOSS) [9] and the bag-of-features framework (TSBF) [10] classifiers. Ensemble-based classifiers combine separate classifiers into one model to reach a higher classification accuracy such as the elastic ensemble (PROP) [11], the shapelet ensemble (SE) [12], and the collective of transform-based ensemble (COTE) [12] classifiers.

Convolutional neural network (CNN) based classifiers have advantages over other classification methods because CNNs provide the classifier with a preprocessing mechanism within the model. Examples are the multi-channel CNN (MC-CNN)

TABLE I: Comparison of GRU and LSTM Computational Elements.

Comparison	LSTM	GRU
number of gates	3	2
number of activations	2	1
state memory cell	Yes	No
number of weight matrices	8	6
number of bias vectors	3	4
number of elementwise multiplies	3	3
number of matrix multiplies	8	6

classifier [13], the multi-layered perceptron (MLP) [4], the fully convolutional network (FCN) [4] and, specifically, the residual network (ResNet) [4].

The present paper focuses on the recurrent neural network based classification approaches such as LSTM-FCN [5] and ALSTM-FCN [5]. These models combine both temporal CNNs and long short-term memory (LSTM) models to provide the classifier with both feature extraction and time dependencies through the dataset during the classification process. These models use additional support algorithms such as attention and fine-tuning algorithms to enhance the LSTM learning due to its complex structure and data requirements.

This paper studies whether the use of gated-recurrent units (GRUs) can improve the hybrid classifiers listed above. We create the GRU-FCN by replacing the LSTM with a GRU in the LSTM-FCN [5]. Like the LSTM-FCN, our model does not require feature engineering or data preprocessing before the training or testing stages. The GRU is able to learn the temporal dependencies within the dataset. Moreover, the GRU has a smaller block architecture and shows comparable performance to the LSTM without need for additional algorithms to support the model.

Although it is difficult to determine the best classifier for all time series types, the proposed model seeks to achieve equivalent accuracy to state-of-the-art classification models in univariate time series classification. Following [4] and [5], our tests use the UCR time series classification archive benchmark [14] to compare our model with other state-of-the-art univariate time series classification models. Our model achieved higher classification performance on several datasets compared to other state-of-the-art classification models.

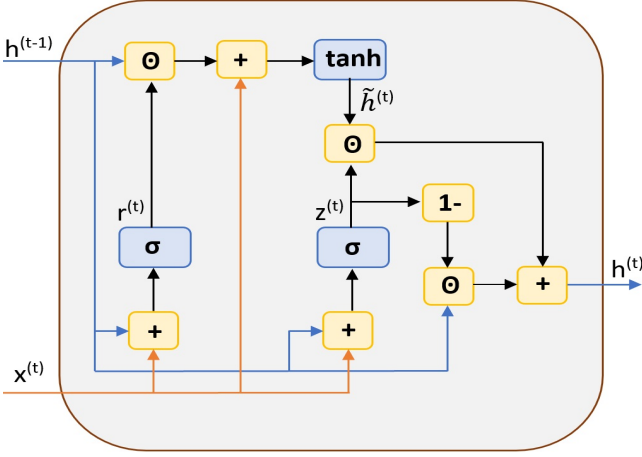


Fig. 1: Block architecture for an unrolled GRU.

II. MODEL COMPONENTS

A. Gated Recurrent Unit (GRU)

The gated recurrent unit (GRU) was introduced in [15] as another type of gate-based recurrent unit which has a smaller architecture and comparable performance to the LSTM unit. The GRU consists of two gates: reset and update. The architecture of an unrolled GRU block is shown in Fig. 1. $r^{(t)}$ and $z^{(t)}$ denote the values of the reset and update gates at time step t , respectively. $x_i \in \mathbb{R}^n$ is a 1D input vector to the GRU block at time step t . $\tilde{h}^{(t)}$ is the output candidate of the GRU block. $h^{(t-1)}$ is the recurrent GRU block output of time step $t-1$ and the current output at time t is $h^{(t)}$. Assuming a one-layer GRU, the reset gate, update gate, output candidate, and GRU output are calculated as follows [15]:

$$z^{(t)} = \sigma(W_{zx}x^{(t)} + U_{zh}h^{(t-1)} + b_z) \quad (1)$$

$$r^{(t)} = \sigma(W_{rx}x^{(t)} + U_{rh}h^{(t-1)} + b_r) \quad (2)$$

$$\tilde{h}^{(t)} = \tanh(W_x x^{(t)} + U_h(r^{(t)} \odot h^{(t-1)} + b)) \quad (3)$$

$$h^{(t)} = (1 - z^{(t)}) \odot h^{(t-1)} + z^{(t)} \odot \tilde{h}^{(t)} \quad (4)$$

Where W_{zx} , W_{rx} , and W_x are the feedforward weights and U_{hz} , U_{hr} , and U_h are the recurrent weights of the update gate, reset gate, and output candidate activation respectively. b_z , b_r , and b are the biases of the update gate, reset gate and the output candidate activation $\tilde{h}^{(t)}$, respectively. Figure 3 shows the GRU architecture with weights and biases made explicit.

Like the RNN and LSTM, the GRU models temporal (sequential) datasets. The GRU uses its previous time step output and current input to calculate the next output. The GRU has the advantage of smaller size over the LSTM. The GRU consists of two gates (reset and update), while the LSTM has three gates: input, output and forget. The GRU has one unit activation, but the LSTM has two unit activations: input-update and output activations. Also, the GRU does not contain the memory state cell which exists in the LSTM model. Thus, the GRU requires fewer trainable parameters, and shorter training time compared to the LSTM. Table I compares GRU and LSTM architecture components.

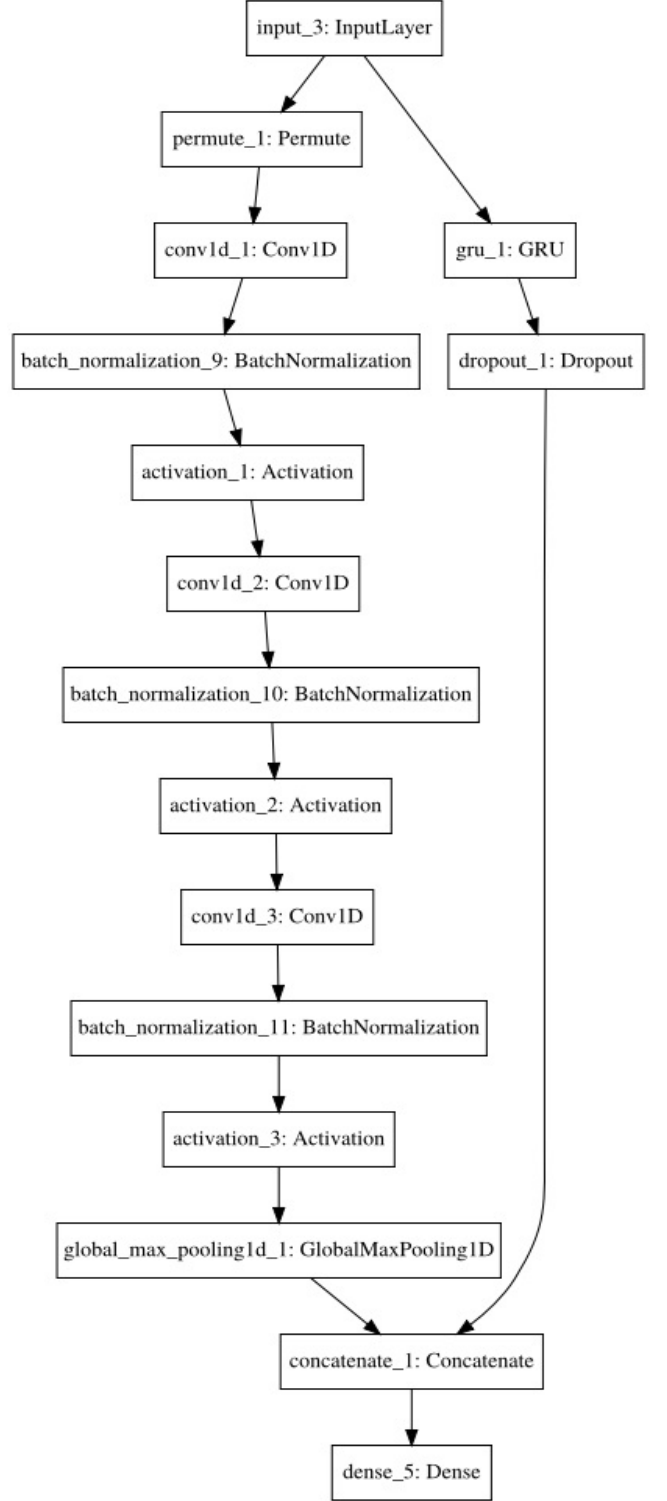


Fig. 2: The proposed model architecture rendered using the Keras visualization tool and modified from [4], [5] architectures.

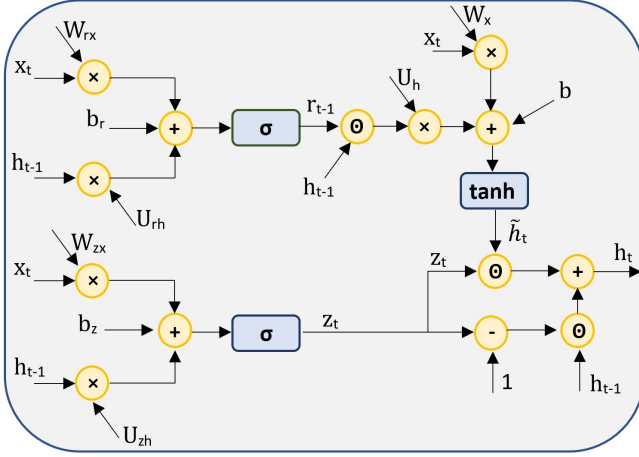


Fig. 3: The GRU architecture showing the weights of each component.

B. Temporal Convolutional Neural Network

The Convolutional Neural Network (CNN), introduced in 1989 [16], utilizes weight sharing over grid-structured datasets such as images and time series [17], [18]. The convolutional layers within the CNN learn to extract complex feature representations from the data with little or no preprocessing. The temporal FCN consists of many layers of convolutional blocks that may have different or same kernel sizes, followed by a dense layer softmax classifier. For time series problems, the values of each convolutional block in the FCN, are calculated as follows [4]:

$$y_i = W_i * x_i + b_i \quad (5)$$

$$z_i = BN(y) \quad (6)$$

$$out_i = ReLU(z) \quad (7)$$

where $x_i \in \mathbb{R}^n$ is a 1D input vector which represents a time series segment, W_i is the 1D convolutional kernel of weights, b_i is the bias, and y is the output vector of the convolutional block i . z_i is the intermediate result after applying batch normalization [19] on the convolutional block which then is passed to the rectified linear unit *ReLU* [20] to calculate the output of the convolutional layer out_i .

III. MODEL ARCHITECTURE

As stated in the introduction, our model replaces the LSTM with a GRU in a hybrid gated-FCN. Our model is based on the framework introduced in [4], [5]. The proposed architecture actual implementation is shown in Figure 2. The architecture has two parallel parts: a GRU and a temporal FCN. Our model uses three layers FCN architecture proposed in [4]. We also used the global average pooling layer to interpret the classes and to reduce the number of trainable parameters comparing to the fully connected layer, without any sacrifice in the accuracy. The FCN 1D kernel sizes are 128, 256, and 128 in each convolutional layer, respectively. The weights were initialized using the He uniform variance scaling initializer [21]. In addition, we used the GRU instead of LSTMs that were used in [5] models to reduce the number

of trainable parameters, memory, and training time. Moreover, we removed the masking and any extra supporting algorithms such as an attention mechanism, and fine-tuning that were used in the LSTM-FCN and ALSTM-FCN models [5]. The GRU is unfolded by eight unfolds as used in [5] for univariate time series. The hyperbolic tangent (*tanh*) function used as the unit activation and the hard-sigmoid (*hardSig*) function [22] is used as the recurrent activation (gate activation) of the GRU architecture. The weights were initialized using the *glorot_uniform* initializer [23], [24] and the biases were initialized to zero. The input was fitted using the concept used in [5] to fit an input to a recurrent unit. We used the Adam optimization function [25] with $\beta_1 = 0.9$, $\beta_2 = 0.999$ and initial learning rate $\alpha = 0.01$. The learning rate α was reduced by a factor of 0.8 every 100 training steps until it reached the minimum rate $\alpha = 0.0001$. The dense layer uses the softmax classifier [26] using the categorical crossentropy loss function [18]. The number of epochs varies between 400 to 1200. In this paper our goal is to make a fair comparison between the LSTM-based model and our GRU-based model. Thus, we used the same number of epochs that was assigned by the original LSTM-FCN model [5] for each univariate time series.

The input to the model is the raw dataset without applying any normalizations or feature engineering. The FCN is responsible for feature extraction from the time series [4] and the GRU enables the model to learn temporal dependencies within the time series. Therefore the model learns both the features and temporal dependencies to predict the correct class for each training example.

IV. METHOD AND RESULTS

We implemented our model by modifying the original LSTM-FCN [5] implementation which we found on github <https://github.com/titu1994/LSTM-FCN>. We found that the fine-tuning algorithm has not been applied in the actual LSTM-FCN and ALSTM-FCN implementation on source code github which shared by the authors [5]. In addition, the LSTM-FCN [5] authors used a permutation algorithm for fitting the input to the FCN part which was not mentioned in their literature. Therefore, we re-generated the actual LSTM-FCN and ALSTM-FCN implementations to record the results based on their actual code implementation. The Keras API [24] with TensorFlow backend [27] were used in the implementation of the LSTM-FCN, ALSTM-FCN and GRU-FCN models. The source code of our GRU-FCN implementation can be found on github: <https://github.com/NellyElsayed/GRU-FCN-model-for-univariate-time-series-classification>. We tested our model on the UCR time series archive [14] as one of the standard benchmarks for time series classification. We used 44 of the 85 different time series datasets. They were divided into training and testing sets. The 44 datasets have different types of collected sources: 13 datasets of image source, 3 spectro source, 4 simulated source, 11 sensor source, 9 motion source, and 4 ECG source. The number of classes in each time series, the length of both the training and test sets are shown in Table II based on the datasets description in [14]. Table II

TABLE II: UCR 44 dataset descriptions based on [14] and its usage in GRU-FCN implementation based on [5].

Dataset	Type	# Classes	Train size	Test size	Length	# epochs	Train Batch	Test Batch
Adiac	Image	37	390	391	176	4000	128	128
Beef	Spectro	5	30	30	470	8000	64	64
CBF	Simulated	3	30	900	128	2000	32	128
ChlorineConc	Sensor	3	467	3840	166	2000	128	128
CinCECGTorso	Sensor	4	40	1380	1639	500	128	128
Coffee	Spectro	2	28	28	286	500	64	64
CricketX	Motion	12	390	390	300	2000	128	128
CricketY	Motion	12	390	390	300	2000	128	128
CricketZ	Motion	12	390	390	300	2000	64	128
DiatomSizeR	Image	4	16	306	345	2000	64	64
ECGFiveDays	ECG	2	23	861	136	2000	128	128
FaceAll	Image	14	560	1690	131	2000	128	128
FaceFour	Image	4	24	88	350	2000	128	128
FacesUCR	Image	14	200	2050	131	2000	128	128
FiftyWords	Image	50	450	455	270	2000	128	128
Fish	Image	7	175	175	463	2000	128	128
GunPoint	Motion	2	50	150	150	2000	128	128
Haptics	Motion	5	155	308	1092	2000	128	128
InlineSkate	Motion	7	100	550	1882	2000	128	128
ItalyPower	Sensor	2	67	1029	24	2000	64	128
Lightning2	Sensor	2	60	61	637	4000	128	128
Lightning7	Sensor	7	70	73	319	3000	32	32
Mallat	Simulated	8	55	2345	1024	2500	128	128
MedicalImages	Image	10	381	760	99	2000	64	128
MoteStrain	Sensor	2	20	1252	84	2000	128	128
NonInvThorax1	ECG	42	1800	1965	750	2000	128	128
NonInvThorax2	ECG	42	1800	1965	750	2000	128	128
OliveOil	Spectro	4	30	30	570	6000	64	128
OSULeaf	Image	6	200	242	427	2000	64	128
SonyAIBORobot	Sensor	2	20	601	70	2000	64	128
SonyAIBORobotII	Sensor	2	27	953	65	2000	64	128
StarLightCurves	Sensor	3	1000	8236	1024	2000	64	64
SwedishLeaf	Image	15	500	625	128	8000	64	64
Symbols	Image	6	25	995	398	2000	64	64
SyntheticControl	Simulated	6	300	300	60	4000	16	128
Trace	Sensor	4	100	100	275	1000	64	128
TwoLeadECG	ECG	2	23	1139	82	2000	64	64
TwoPatterns	Simulated	4	1000	4000	128	2000	32	128
UWaveX	Motion	8	896	3582	315	2000	64	16
UWaveY	Motion	8	896	3582	315	2000	64	64
UWaveZ	Motion	8	896	3582	315	2000	64	64
Wafer	Sensor	2	1000	6164	152	1500	64	64
WordSynonyms	Image	25	267	638	270	1500	64	64
Yoga	Image	2	300	3000	426	1000	128	128

also shows the number of epochs through training, and the batch sizes of the training and testing stages.

We compared our GRU-FCN with several state-of-the-art time series methods that also were studied in [4] and [5]. These included FCN [4] which is based on a fully convolutional network, LSTM-FCN [5], ALSTM-FCN [5], that are based on long short-term memory and fully convolutional networks, ResNet [4] which based on convolutional residual networks, MCNN [13] that is based on convolutional networks, MLP [4] which based on multilayer perceptrons, COTE [12] which based on transformation ensembles, DTW [28] that is based on a weighted dynamic time warping mechanism, PROP [11] which is based on elastic distance measures, BOSS [9] that based on noise reduction in the time series representation, and SE [12] that based on Shapelet ensemble. Our model shows the overall highest number of being the best classifier for 20 time series out of 44. Our model also shows the overall smallest classification error, arithmetic average rank, and mean per-class classification error (MPCE) compared to the other models as shown in Table III.

We divided the 44 UCR datasets based on the source of obtaining each dataset to show the accuracy of each classification model over different time series of same data source type. We did so to analyze the different classifiers over the different data source types separately. Figure 5 shows the accuracy of each classification model over image source datasets classification where the GRU-FCN shows the highest number of the highest classification accuracy compare to the state-of-the-art classifiers. Figure 6 shows the accuracy of each classification method on the spectro source datasets, where our GRU-FCN accuracy outperforms the state-of-the-art classifiers over all of the spectro source datasets. Figures 7, 8, 9, and 10 show the accuracy of each classification method on simulated, sensor, motion, and ECG source datasets. For the ECG source datasets, our model outperforms all the univariate time series state-of-the-art models except for the ECGFiveDays dataset. However, by increasing the kernel size of the FCN part in the GRU-FCN, the model can reach the highest accuracy in this dataset classification.

We evaluated our model using the Mean Per-Class Error

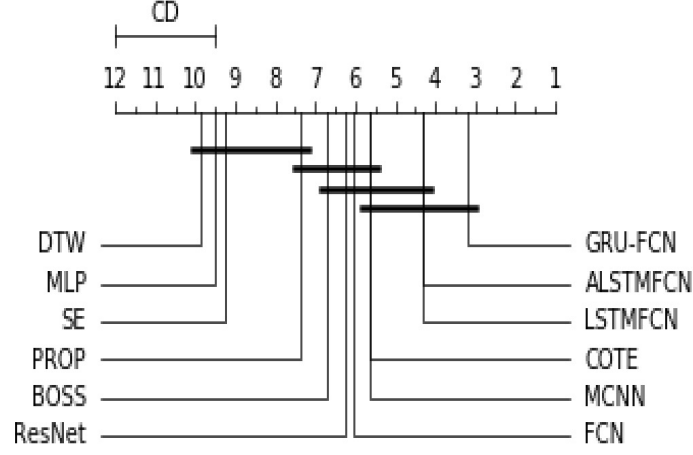


Fig. 4: Critical difference diagram based on arithmetic mean of model ranks.

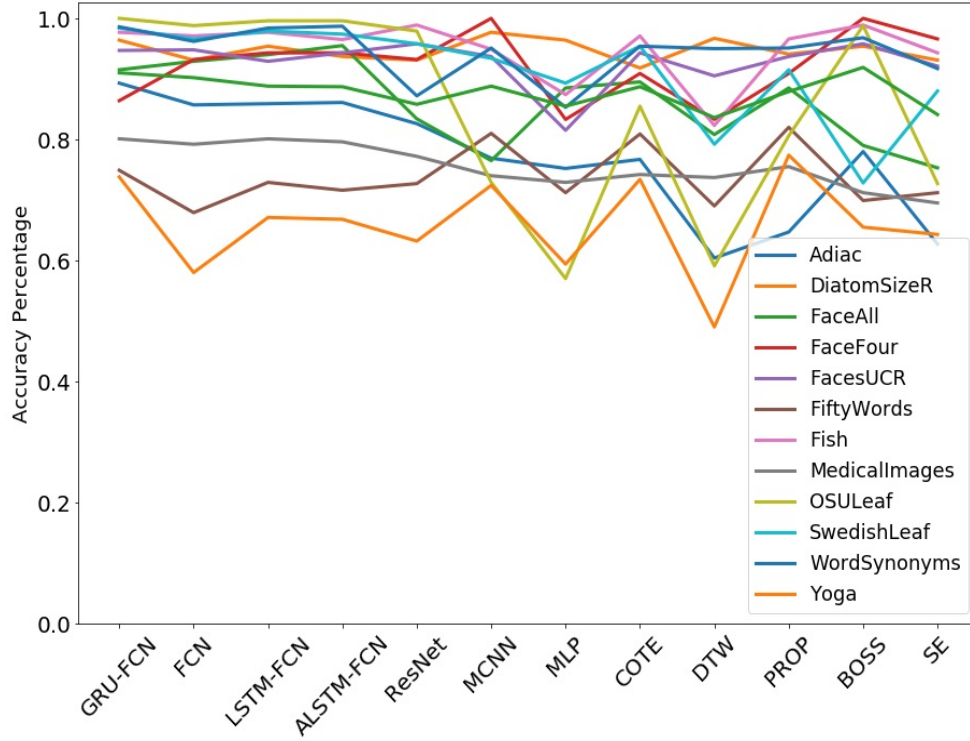


Fig. 5: Classification accuracy over the image source datasets.

(MPCE) used in [4] to evaluate performance of a classification method over multiple datasets. The MPCE for a given model is calculated based on the per-class error (PCE) as follows:

$$\text{PCE}_m = \frac{e_m}{c_m} \quad (8)$$

$$\text{MPCE} = \frac{1}{M} \sum_{m=1}^M \text{PCE}_m \quad (9)$$

where e_m is the error rate for dataset m consisting of c_m classes. M is the number of tested datasets.

Table III shows the MPCE value for our GRU-FCN and other state-of-the-art models on the UCR benchmark datasets. The results obtained by implementing GRU-FCN and regenerating LSTM-FCN, and ALSTM models based on their

actual implementation on github. For the other models, we obtained the results from their own publications. Our GRU-FCN has the smallest MPCE value compared to the other state-of-the-art classification models. This means that generally our GRU-FCN model performance across the different datasets is higher than the other state-of-the-art models.

Figure 4 shows the critical difference diagram [29] for Nemenyi or Bonferroni-Dunn test [30] with $\alpha = 0.05$ on our GRU-FCN and the state-of-the-art models based on the ranks arithmetic mean on the UCR benchmark datasets. This graph shows the significant classification accuracy improvement of our GRU-FCN compared to the other state-of-the-art models.

Table IV shows the Wilcoxon signed-rank test which provides the overall accuracy evidence of each of the eleven

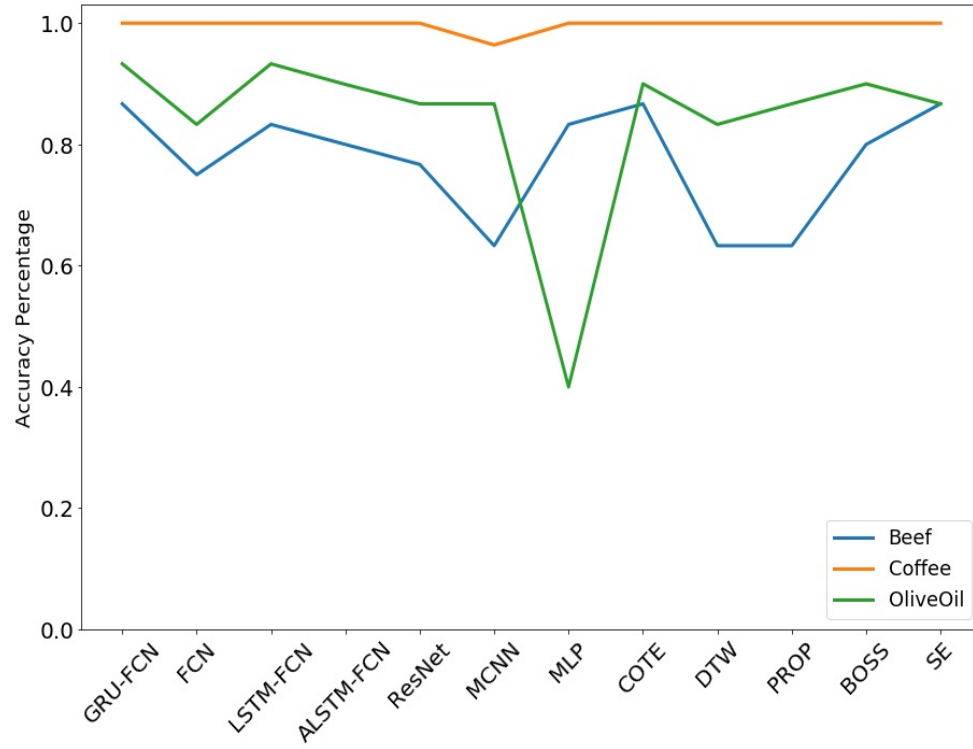


Fig. 6: Classification accuracy over the spectro source datasets.

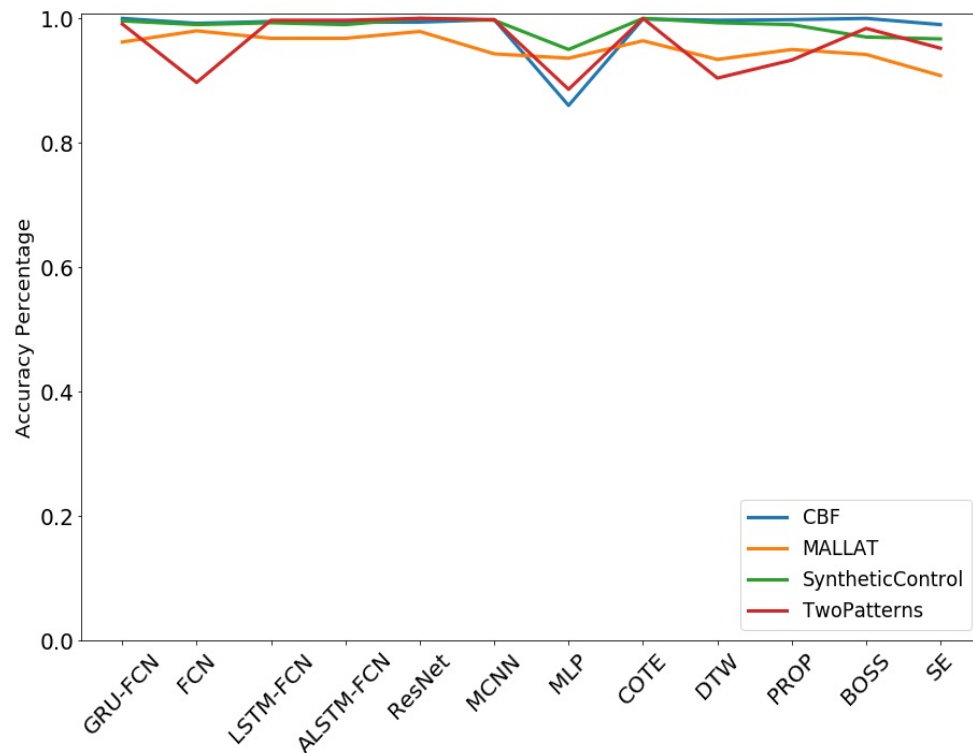


Fig. 7: Classification accuracy over the simulated source datasets.

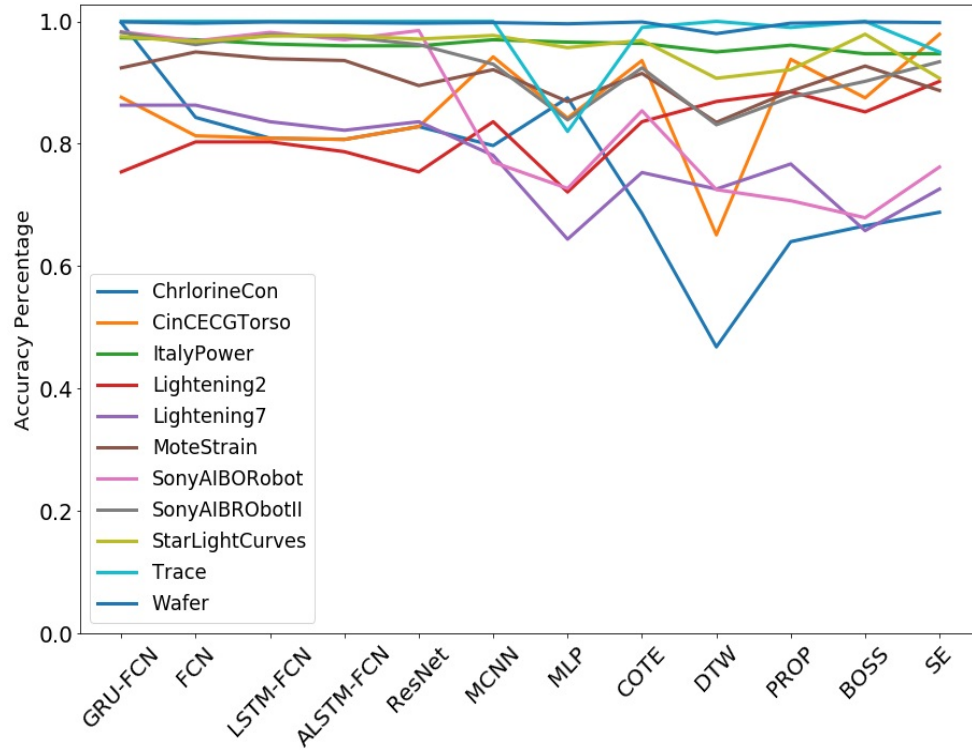


Fig. 8: Classification accuracy over the sensor source datasets.

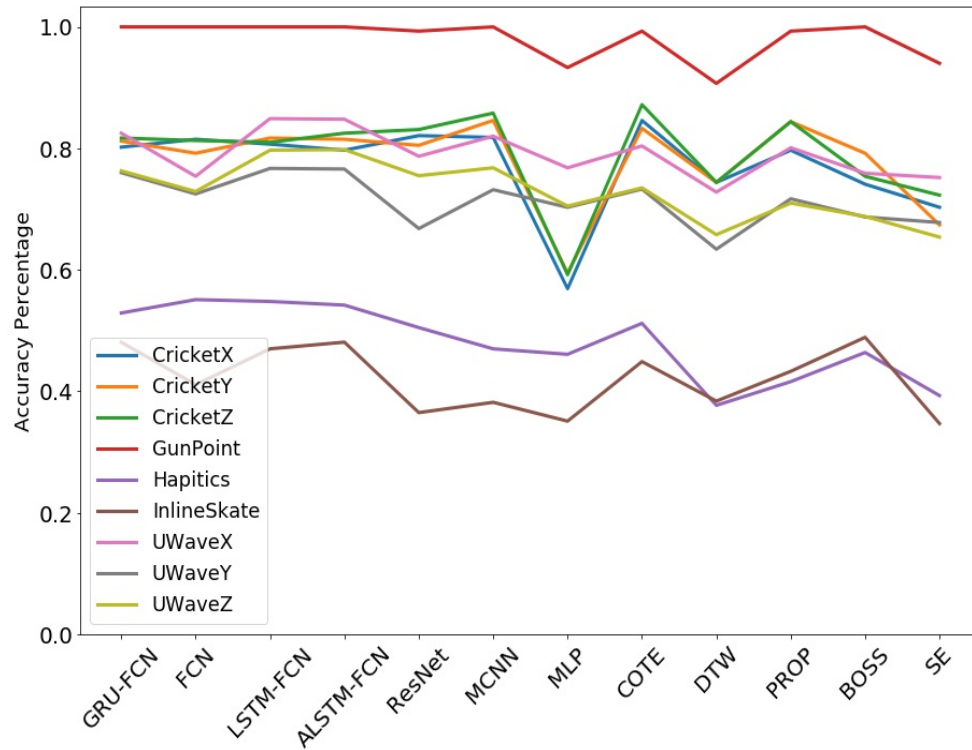


Fig. 9: Classification accuracy over the motion source datasets.

TABLE III: Classification testing error percentage and rank for 44 time series datasets from the UCR benchmark.

Dataset	Classification Method and Error Percentage											
	GRU-FCN	FCN	LSTMFCN	ALSTMFCN	ResNet	MCNN	MLP	COTE	DTW	PROP	BOSS	SE
Adiac	0.107	0.143	0.141	0.139	0.174	0.231	0.248	0.233	0.396	0.353	0.22	0.373
Beef	0.133	0.250	0.167	0.200	0.233	0.367	0.167	0.133	0.367	0.367	0.2	0.133
CBF	0	0.008	0.005	0.006	0.006	0.002	0.140	0.001	0.003	0.002	0	0.010
ChlorineCon	0.002	0.157	0.191	0.193	0.172	0.203	0.125	0.314	0.532	0.360	0.334	0.312
CinCEGTorso	0.124	0.187	0.191	0.193	0.172	0.058	0.158	0.064	0.349	0.062	0.125	0.021
Coffee	0	0	0	0	0	0.036	0	0	0	0	0	0
CricketX	0.198	0.185	0.193	0.203	0.179	0.182	0.431	0.154	0.256	0.203	0.259	0.297
CricketY	0.188	0.208	0.183	0.185	0.195	0.154	0.405	0.167	0.256	0.156	0.208	0.326
CricketZ	0.183	0.187	0.190	0.175	0.169	0.142	0.408	0.128	0.256	0.156	0.246	0.277
DiatomSizeR	0.036	0.069	0.046	0.063	0.069	0.023	0.036	0.082	0.033	0.059	0.046	0.069
ECGFiveDays	0.007	0.010	0.012	0.012	0.045	0	0.030	0	0.232	0.178	0	0.055
FaceAll	0.085	0.071	0.060	0.045	0.166	0.235	0.115	0.105	0.192	0.115	0.21	0.247
FaceFour	0.136	0.068	0.057	0.057	0.068	0	0.167	0.091	0.167	0.091	0	0.034
FacesUCR	0.053	0.052	0.071	0.057	0.042	0.063	0.185	0.057	0.095	0.063	0.042	0.079
Fiftywords	0.251	0.321	0.271	0.284	0.273	0.19	0.288	0.191	0.31	0.180	0.301	0.288
fish	0.023	0.029	0.023	0.035	0.011	0.051	0.126	0.029	0.177	0.034	0.011	0.057
GunPoint	0	0	0	0	0.007	0	0.067	0.007	0.093	0.007	0	0.060
Haptics	0.471	0.449	0.452	0.458	0.495	0.530	0.539	0.488	0.623	0.584	0.536	0.607
InlineSkate	0.519	0.589	0.530	0.519	0.635	0.618	0.649	0.551	0.616	0.567	0.511	0.653
ItalyPower	0.027	0.030	0.037	0.040	0.04	0.030	0.034	0.036	0.050	0.039	0.053	0.053
Lightning2	0.246	0.197	0.197	0.213	0.246	0.164	0.279	0.164	0.131	0.115	0.148	0.098
Lightning7	0.137	0.137	0.164	0.178	0.164	0.219	0.356	0.247	0.274	0.233	0.342	0.274
MALLAT	0.038	0.020	0.032	0.032	0.021	0.057	0.064	0.036	0.066	0.050	0.058	0.092
MedicalImages	0.199	0.208	0.199	0.204	0.228	0.26	0.271	0.258	0.263	0.245	0.288	0.305
MoteStrain	0.076	0.05	0.061	0.064	0.105	0.079	0.131	0.085	0.165	0.114	0.073	0.113
NonInvThorax1	0.037	0.039	0.037	0.037	0.052	0.064	0.058	0.093	0.21	0.178	0.161	0.174
NonInvThorax2	0.042	0.045	0.043	0.048	0.049	0.060	0.057	0.073	0.135	0.112	0.101	0.118
OliveOil	0.067	0.167	0.067	0.101	0.133	0.133	0.6	0.1	0.167	0.133	0.100	0.133
OSULeaf	0	0.012	0.004	0.004	0.021	0.271	0.430	0.145	0.409	0.194	0.012	0.273
SonyAIBORobot	0.017	0.032	0.018	0.030	0.015	0.230	0.273	0.146	0.275	0.293	0.321	0.238
SonyAIBORobotII	0.018	0.038	0.022	0.025	0.038	0.070	0.161	0.076	0.169	0.124	0.098	0.066
StarLightCurves	0.025	0.033	0.024	0.023	0.029	0.023	0.043	0.031	0.093	0.079	0.021	0.093
SwedishLeaf	0.016	0.034	0.021	0.026	0.042	0.066	0.107	0.046	0.208	0.085	0.272	0.12
Symbols	0.014	0.038	0.016	0.013	0.128	0.049	0.147	0.046	0.05	0.049	0.032	0.083
SyntheticControl	0.004	0.010	0.007	0.010	0	0.003	0.050	0	0.007	0.010	0.030	0.033
Trace	0	0	0	0	0	0	0.18	0.01	0	0.01	0	0.05
TwoLeadECG	0	0	0.001	0.001	0	0.001	0.147	0.015	0	0	0.004	0.029
TwoPatterns	0.009	0.103	0.003	0.003	0	0.002	0.114	0	0.096	0.067	0.016	0.048
UWaveX	0.175	0.246	0.151	0.152	0.213	0.18	0.232	0.196	0.272	0.199	0.241	0.248
UWaveY	0.240	0.275	0.233	0.234	0.332	0.268	0.297	0.267	0.366	0.283	0.313	0.322
UWaveZ	0.237	0.271	0.203	0.202	0.245	0.232	0.295	0.265	0.342	0.290	0.312	0.346
wafer	0.001	0.003	0.001	0.002	0.003	0.002	0.004	0.001	0.020	0.003	0.001	0.002
WordSynonyms	0.262	0.42	0.329	0.332	0.368	0.276	0.406	0.266	0.510	0.226	0.345	0.357
yoga	0.090	0.098	0.112	0.113	0.142	0.112	0.145	0.113	0.164	0.121	0.081	0.159
no. best (out of 44)	20	8	9	6	7	6	1	8	3	4	12	4
Arithmetic AVG Rank	3.193	6.068	4.2954	4.295	6.227	5.636	9.488	5.625	9.875	7.363	6.693	9.238
MPCE	0.0170	0.0207	0.0182	0.0192	0.022	0.0240	0.0400	0.0226	0.0407	0.0299	0.0257	0.0299

TABLE IV: Wilcoxon signed-rank test on GRU-FCN and 10 benchmark model.

[illegible]

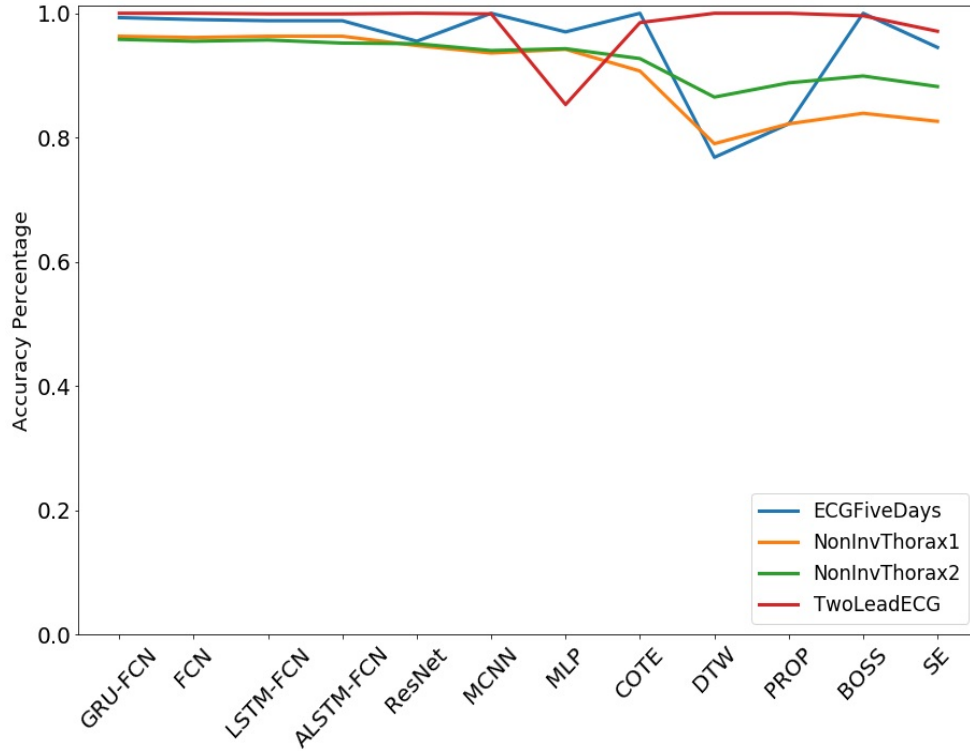


Fig. 10: Classification accuracy over the ECG source datasets.

classification methods.

V. CONCLUSION

The proposed GRU-FCN classification model shows that replacing the LSTM by a GRU enhances the classification accuracy without needing extra algorithm enhancements such as fine-tuning or attention algorithms. The GRU also has a smaller architecture requiring fewer computations than the LSTM. Furthermore, the proposed GRU-FCN classification model achieves the performance of state-of-the-art models and has the highest average arithmetic ranking and the lowest mean per-class error (MPCE) through time series datasets classification of the UCR benchmark compared to the state-of-the-art models. Moreover, the proposed GRU-FCN achieved the highest accuracy in all the spectro source datasets and in almost all the ECG source datasets comparing to the state-of-the-art models. Therefore, replacing the LSTM by GRU in the LSTM-FCN for univariate time series classification can improve the classification with smaller model architecture.

REFERENCES

- [1] J. D. Hamilton, *Time series analysis*. Princeton University Press, Princeton, NJ, 1994, vol. 2.
- [2] H. Sohn and C. R. Farrar, "Damage diagnosis using time series analysis of vibration signals," *Smart Materials and Structures*, vol. 10, no. 3, p. 446, 2001.
- [3] M. Gul and F. N. Catbas, "Statistical pattern recognition for structural health monitoring using time series modeling: theory and experimental verifications," *Mechanical Systems and Signal Processing*, vol. 23, no. 7, pp. 2192–2204, 2009.
- [4] Z. Wang, W. Yan, and T. Oates, "Time series classification from scratch with deep neural networks: a strong baseline," in *Neural Networks (IJCNN), 2017 International Joint Conference on*. IEEE, 2017, pp. 1578–1585.
- [5] F. Karim, S. Majumdar, H. Darabi, and S. Chen, "LSTM fully convolutional networks for time series classification," *IEEE Access*, vol. 6, pp. 1662–1669, 2018.
- [6] A. Amei, W. Fu, and C.-H. Ho, "Time series analysis for predicting the occurrences of large scale earthquakes," *International Journal of Applied Science and Technology*, vol. 2, no. 7, 2012.
- [7] J. Rotton and J. Frey, "Air pollution, weather, and violent crimes: concomitant time-series analysis of archival data," *Journal of Personality and Social Psychology*, vol. 49, no. 5, p. 1207, 1985.
- [8] E. Keogh and C. A. Ratanamahatana, "Exact indexing of dynamic time warping," *Knowledge and Information Systems*, vol. 7, no. 3, pp. 358–386, 2005.
- [9] P. Schäfer, "The BOSS is concerned with time series classification in the presence of noise," *Data Mining and Knowledge Discovery*, vol. 29, no. 6, pp. 1505–1530, 2015.
- [10] M. G. Baydogan, G. Runger, and E. Tuv, "A bag-of-features framework to classify time series," *IEEE Transactions on Pattern Analysis and Machine Intelligence*, vol. 35, no. 11, pp. 2796–2802, 2013.
- [11] J. Lines and A. Bagnall, "Time series classification with ensembles of elastic distance measures," *Data Mining and Knowledge Discovery*, vol. 29, no. 3, pp. 565–592, 2015.
- [12] A. Bagnall, J. Lines, J. Hills, and A. Bostrom, "Time-series classification with COTE: the collective of transformation-based ensembles," *IEEE Transactions on Knowledge and Data Engineering*, vol. 27, no. 9, pp. 2522–2535, 2015.
- [13] Z. Cui, W. Chen, and Y. Chen, "Multi-scale convolutional neural networks for time series classification," *arXiv preprint arXiv:1603.06995*, 2016.
- [14] Y. Chen, E. Keogh, B. Hu, N. Begum, A. Bagnall, A. Mueen, and G. Batista. (2015, July) The UCR time series classification archive. [Online]. Available: http://www.cs.ucr.edu/~eamonn/time_series_data/
- [15] J. Chung, C. Gulcehre, K. Cho, and Y. Bengio, "Empirical evaluation of gated recurrent neural networks on sequence modeling," *arXiv preprint arXiv:1412.3555*, 2014.
- [16] Y. LeCun, B. Boser, J. S. Denker, D. Henderson, R. E. Howard, W. Hubbard, and L. D. Jackel, "Backpropagation applied to handwritten zip code recognition," *Neural Computation*, vol. 1, no. 4, pp. 541–551, 1989.
- [17] Y. LeCun and Y. Bengio, "Convolutional networks for images, speech,

- and time series,” in *The Handbook of Brain Theory and Neural Networks*. MIT Press, 1995, pp. 255–258.
- [18] I. Goodfellow, Y. Bengio, A. Courville, and Y. Bengio, *Deep Learning*. MIT press Cambridge, 2016, vol. 1.
 - [19] S. Ioffe and C. Szegedy, “Batch normalization: Accelerating deep network training by reducing internal covariate shift,” *arXiv preprint arXiv:1502.03167*, 2015.
 - [20] V. Nair and G. E. Hinton, “Rectified linear units improve restricted Boltzmann machines,” in *Proceedings of the 27th International Conference on Machine Learning (ICML-10)*, 2010, pp. 807–814.
 - [21] K. He, X. Zhang, S. Ren, and J. Sun, “Delving deep into rectifiers: surpassing human-level performance on imagenet classification,” in *Proceedings of the IEEE International Conference on Computer Vision*, 2015, pp. 1026–1034.
 - [22] C. Gulcehre, M. Moczulski, M. Denil, and Y. Bengio, “Noisy activation functions,” in *International Conference on Machine Learning*, 2016, pp. 3059–3068.
 - [23] X. Glorot and Y. Bengio, “Understanding the difficulty of training deep feedforward neural networks,” in *Proceedings of the Thirteenth International Conference on Artificial Intelligence and Statistics*, 2010, pp. 249–256.
 - [24] F. Chollet *et al.*, “Keras,” <https://keras.io>, 2015.
 - [25] D. P. Kingma and J. Ba, “Adam: A method for stochastic optimization,” *arXiv preprint arXiv:1412.6980*, 2014.
 - [26] N. M. Nasrabadi, “Pattern recognition and machine learning,” *Journal of Electronic Imaging*, vol. 16, no. 4, p. 049901, 2007.
 - [27] M. Abadi, A. Agarwal, P. Barham, E. Brevdo, Z. Chen, C. Citro, G. S. Corrado, A. Davis, J. Dean, M. Devin, S. Ghemawat, I. Goodfellow, A. Harp, G. Irving, M. Isard, Y. Jia, R. Jozefowicz, L. Kaiser, M. Kudlur, J. Levenberg, D. Mané, R. Monga, S. Moore, D. Murray, C. Olah, M. Schuster, J. Shlens, B. Steiner, I. Sutskever, K. Talwar, P. Tucker, V. Vanhoucke, V. Vasudevan, F. Viégas, O. Vinyals, P. Warden, M. Wattenberg, M. Wicke, Y. Yu, and X. Zheng, “TensorFlow: Large-scale machine learning on heterogeneous systems,” 2015, software available from tensorflow.org. [Online]. Available: <https://www.tensorflow.org/>
 - [28] Y.-S. Jeong, M. K. Jeong, and O. A. Omitaomu, “Weighted dynamic time warping for time series classification,” *Pattern Recognition*, vol. 44, no. 9, pp. 2231–2240, 2011.
 - [29] J. Demšar, “Statistical comparisons of classifiers over multiple data sets,” *Journal of Machine Learning Research*, vol. 7, no. Jan, pp. 1–30, 2006.
 - [30] T. Pohlert, “The pairwise multiple comparison of mean ranks package (PMCMR),” *R Package*, vol. 27, 2014.